

## EFFECT OF SELECTED ALLOYING ELEMENTS ON THE SOFT-MAGNETIC AND MECHANICAL PROPERTIES OF INJECTION-CAST $\text{Fe}_{61}\text{Co}_{10}\text{Y}_8\text{Me}_1\text{B}_{20}$ ALLOYS (Me = Nb, W OR Mo)

Properties of amorphous alloys differ from each other when they are produced at different cooling rates and from different chemical compositions. This paper presents studies of the magnetic and mechanical properties of  $\text{Fe}_{61}\text{Co}_{10}\text{Y}_8\text{Nb}_1\text{B}_{20}$ ,  $\text{Fe}_{61}\text{Co}_{10}\text{Y}_8\text{W}_1\text{B}_{20}$  and  $\text{Fe}_{61}\text{Co}_{10}\text{Y}_8\text{Mo}_1\text{B}_{20}$  alloys, in the form of plates, produced by the injection of liquid alloy into a copper mould. Based on the performed studies, it was found that the substitution of 1% non-magnetic additive into the alloy composition had little effect, as regards the values of saturation magnetization ( $M_s$ ) and Curie temperature ( $T_c$ ). However, in the case of the coercive field, the sample with the W addition had a value almost half that of the other two alloys. For all of the studied alloys, the microhardness was about 1180  $\mu\text{Hv}100$ , i.e. significantly higher than for the same materials in the crystalline state.

*Keywords:* magnetic properties, mechanical properties, abrasion resistance, microhardness, Curie temperature

### 1. Introduction

One of the first types of metallic glass to be produced on an industrial scale was in the form of thin ribbons with thicknesses of less than a few micrometres [1-3]. Initially, mostly due to the dimensions of these glass samples, industrial applications have been limited. However, the iron-based ribbons were characterized by very good soft magnetic properties [4-6]. At present, cores for low-loss transformers are being made using this type of ribbon. When operating under ‘no-load’ conditions, these cores don’t absorb power; when under ‘load’ their physical dimensions don’t change, which implies that magnetostriction is close to zero [5]. An ideal material to use for transformer cores would be bulk amorphous material exhibiting similar properties to the aforementioned amorphous ribbons. In recent years, many attempts have been made to create a production technique for bulk amorphous alloys [7-9]. The story of the bulk amorphous alloys began in 1989 when A. Inoue from Tohoku University in Japan, together with his co-workers, developed three fundamental criteria for facilitating the reproducible manufacture of bulk amorphous alloys [8]. Inoue found that, in order to make bulk amorphous alloy, certain conditions have to be fulfilled: (1) The alloy has to consist of more than three elements, (2) The radii of the component elements must differ by 12%, and (3) There must be negative mixing heat [8]. From that moment, many scientific institutions began to produce bulk amorphous alloys. Various methods of manufacturing were developed, including the most popular methods: suction- and injection-casting [10-15]. An especially interesting group of bulk amorphous alloys is

that exhibiting so-called soft magnetic properties. In the future, this type of alloy could replace the ubiquitous FeSi transformer steel. In addition, the ferromagnetic amorphous alloys possess values of hardness twice as high as those of their crystalline counterparts. Very often, the soft magnetic properties are determined by minor changes in the chemical composition of the alloy [13,15-17]. Therefore investigations into subtle changes in alloy compositions are very important.

In this paper, the results are presented of investigations into the group of alloys:  $\text{Fe}_{61}\text{Co}_{10}\text{Y}_8\text{Me}_1\text{B}_{20}$ , (where: Me = Nb, W or Mo) in the as-cast state. All samples were made by the injection of the molten alloy into a copper die (i.e. the injection-casting method).

### 2. Materials and methods of investigations

The samples of  $\text{Fe}_{61}\text{Co}_{10}\text{Y}_8\text{Me}_1\text{B}_{20}$  alloy (where: Me = Nb, W or Mo) were produced by injecting the molten material into a copper die. The entire production process was carried out under a protective gas atmosphere. The initial ingots of each alloy were made by arc-melting. The weighed alloy components were re-melted several times to ensure the homogeneity of the final alloy. The components used were of high purity: Fe-99.99 at.%, Co-99.99 at.%, Y-99.99 at.%, Nb-99.9999 at.%, W-99.9999 at.%, and Mo-99.9999 at.%; the boron element was added in the form of an alloy of known composition, i.e.:  $\text{Fe}_{45.4}\text{B}_{54.6}$ . The produced samples were produced in the form of plates of thickness approximately 0.5 mm and surface area approximately 100 mm<sup>2</sup>.

\* CZĘSTOCHOWA UNIVERSITY OF TECHNOLOGY, INSTITUTE OF PHYSICS, 69 DĄBROWSKIEGO STR., 42-201 CZĘSTOCHOWA, POLAND

<sup>#</sup> Corresponding author: pietrusiewicz@wip.pcz.pl

The microstructure was investigated by means of a “BRUKER” X-ray diffractometer (CuK $\alpha$ ). The values of the Curie temperature, which define the limit of stability of the ferromagnetic properties, were estimated from analysis of the magnetization versus temperature curves. Magnetization was measured over the temperature range: from room temperature up to 850 K, using a Faraday magnetic balance. Static hysteresis loops were taken using a “LakeShore” magnetometer with vibrating sample. The microhardness of the samples was obtained using a microhardness system with 100 G load (in the form of a pyramid) and pressure was applied for 10 s. Abrasion tests were performed using a “Kulotester” by comparing the abrasion area produced by a rotating zircon ball after a 1 h test.

The aim of this work was to investigate the influence of the alloying element (Me = Nb, W or Mo) on the magnetic and mechanical properties of the Fe<sub>61</sub>Co<sub>10</sub>Y<sub>8</sub>Me<sub>1</sub>B<sub>20</sub> alloy, produced by injection of the molten alloy into a water-cooled copper die.

### 3. Results and discussion

Fig. 1 shows X-ray diffraction patterns for the samples of the Fe<sub>61</sub>Co<sub>10</sub>Y<sub>8</sub>Me<sub>1</sub>B<sub>20</sub> alloys (where: Me = Nb, W or Mo). Only single, broad maxima can be seen, which is typical for materials with a topologically disordered structure, hence characteristic for amorphous materials.

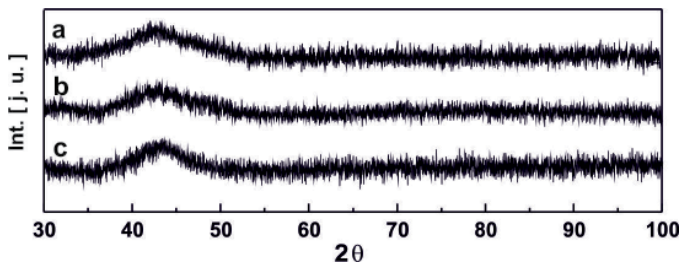


Fig. 1. X-ray diffraction patterns for the samples of the Fe<sub>61</sub>Co<sub>10</sub>Y<sub>8</sub>Me<sub>1</sub>B<sub>20</sub> alloys in the as-cast state (where: Me = Nb (a), W (b), Mo (c))

The Curie temperature ( $T_c$ ) is a very important parameter, describing the thermal stability of the ferromagnetic state in the investigated materials. The respective values of this parameter were found from analysis of the thermomagnetic curves (Fig. 2) using the following relationship:

$$(\mu_0 M_S)^{1/\beta} = (\mu_0 M_0)^{1/\beta} \left(1 - \frac{T}{T_c}\right) \quad (1)$$

where:

$\mu_0 M_0$  – Saturation magnetization at  $T = 0$  K,

$T_c$  – Curie temperature,

$\beta = 0.36$  – Critical factor for the Heisenberg ferromagnet [18].

The values of the Curie temperatures ( $T_c$ ), calculated according to Eq. (1), are gathered in Table 1. The Curie temperature of the alloy was only slightly affected by addition of the: Nb, W or Mo as alloying elements. All of the investigated samples of the

Fe<sub>61</sub>Co<sub>10</sub>Y<sub>8</sub>Me<sub>1</sub>B<sub>20</sub> alloy (where: Me = Nb, W, Mo) possessed similar values of the  $T_c$ , within the method error of  $\pm 5$  K.

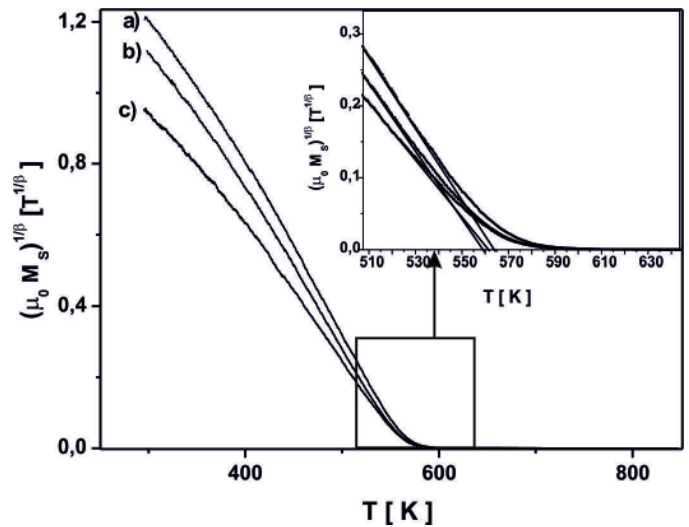


Fig. 2. Thermomagnetic curves obtained for the samples of Fe<sub>61</sub>Co<sub>10</sub>Y<sub>8</sub>Me<sub>1</sub>B<sub>20</sub> alloys in the as-cast state, where: Me = Nb (a), W (b), Mo (c)

TABLE 1

Calculated values of the Curie temperatures of the investigated alloys, obtained from  $(\mu_0 M_S)^{1/\beta}(T)$

Alloy composition	$T_c$ [K]
Fe <sub>61</sub> Co <sub>10</sub> Y <sub>8</sub> Nb <sub>1</sub> B <sub>20</sub>	562
Fe <sub>61</sub> Co <sub>10</sub> Y <sub>8</sub> W <sub>1</sub> B <sub>20</sub>	559
Fe <sub>61</sub> Co <sub>10</sub> Y <sub>8</sub> Mo <sub>1</sub> B <sub>20</sub>	564

The static hysteresis loops obtained from measurements using a magnetometer with vibrating sample (VSM) are shown in Fig. 3, while selected magnetic parameters from analysis of the alloys are presented in Table 2. The alloy featuring Fe<sub>61</sub>Co<sub>10</sub>Y<sub>8</sub>Me<sub>1</sub>B<sub>20</sub> with addition of non-magnetic Nb was found to yield the highest value of  $\mu_0 M_S$ ; However, addition of the elements: W and Mo decreased the saturation magnetization values; this could be caused by antiferromagnetic influences between Mo-Fe or W-Fe [19]. In amorphous materials, the value of the coercive field ( $H_c$ ) (Fig. 4) is correlated with its structure and depends on the local structural relaxation. The values of  $H_c$  for the investigated alloys were found to differ significantly, and, out of the investigated samples, the best soft magnetic parameters, were exhibited by the alloy featuring the addition of W ( $H_c = 24$  A/m).

TABLE 2

Magnetic parameters for the investigated alloys, obtained from analysis of the static hysteresis loops

Alloy composition	As-cast state		Ref.
	$\mu_0 M_S$ [T]	$H_c$ [A/m]	
Fe <sub>61</sub> Co <sub>10</sub> Y <sub>8</sub> Nb <sub>1</sub> B <sub>20</sub>	1.21	56	[10]
Fe <sub>61</sub> Co <sub>10</sub> Y <sub>8</sub> W <sub>1</sub> B <sub>20</sub>	1.19	24	[20][21]
Fe <sub>61</sub> Co <sub>10</sub> Y <sub>8</sub> Mo <sub>1</sub> B <sub>20</sub>	1.17	42	[22]

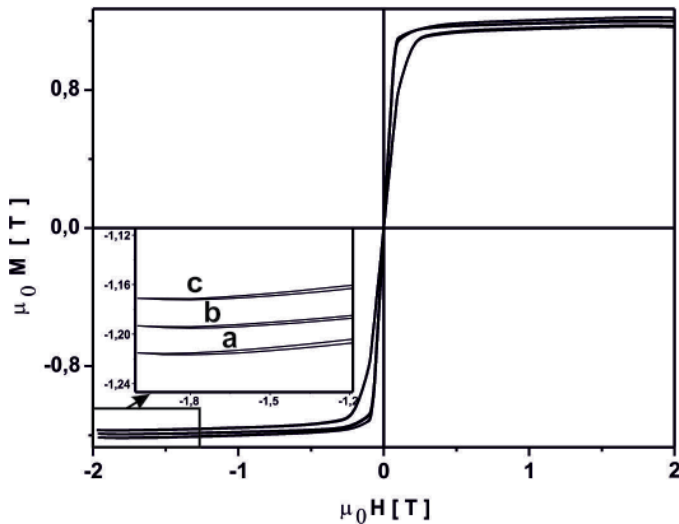


Fig. 3. Static hysteresis loops measured for the investigated samples of  $\text{Fe}_{61}\text{Co}_{10}\text{Y}_8\text{Me}_1\text{B}_{20}$ , where: Me = Nb (a), W (b), Mo (c)

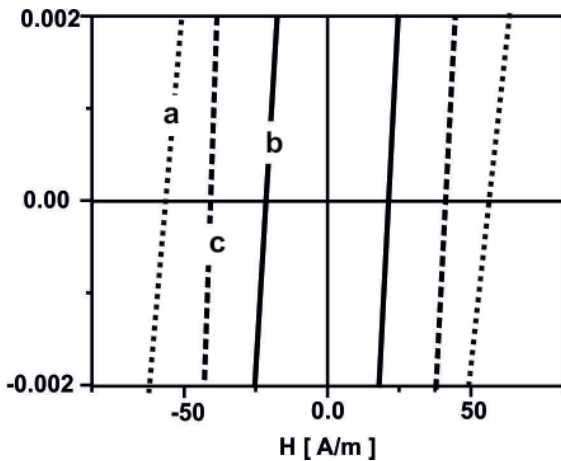


Fig. 4. Magnified origin of M–H system showing a section of the static hysteresis loops with coercivity for the investigated  $\text{Fe}_{61}\text{Co}_{10}\text{Y}_8\text{Me}_1\text{B}_{20}$  alloys where: Me = Nb (a), W (b), Mo (c)

It is well known that the addition of Nb, as an alloying element, eases the crystallization process. This fact, together with the values of magnetic parameters from Table 2, supports the claim that within samples of the  $\text{Fe}_{61}\text{Co}_{10}\text{Y}_8\text{Nb}_1\text{B}_{20}$  alloy, regions with similar chemical configuration could exist, which exhibit, short-range atom ordering.

Regions with variable density on their boundaries could cause blocking of movement of the domain walls, leading to an increase in coercivity to  $H_c = 56 \text{ A/m}$ .

Fig. 5 a shows images of the regions obtained after abrasion tests on the investigated plate-form alloy samples; these abrasion tests were undertaken using a ‘Kulotester’, equipped with a zirconium ball. In Fig. 5 b, an obtained exemplar image is shown for the sample of  $\text{Fe}_{61}\text{Co}_{10}\text{Y}_8\text{Nb}_1\text{B}_{20}$  alloy, which was subjected to a microhardness test using the Vickers method.

Measurements of ‘hardness’ are commonly used in order to quantify the mechanical properties of the metallic glasses. For brittle materials, a significant value of load is used during measurements. The micro-hardness of the investigated alloys was measured using the Vickers method with a load of 100 G.

The iron-based alloys are more covalent and, as such, are more prone to cracking due to their directional atomic bonds [23]. Therefore, during the entry of the indenter into the investigated surface, both shear bands and cracks can be created.

The investigated alloys exhibit low resistance to cracking. This could be connected to their low ductility, as shear bands were not observed around the indentation created during the probing process (Fig. 4b). After application of the 100 G load to the surface of each sample, no visible cracks had been created around the indentation formed during the probing process of the Vickers method (Fig. 4b).

The results of the microhardness and abrasion tests are presented in Table 3. On this basis, it can be stated that the addition of W improved significantly mechanical properties, such as: microhardness and abrasion resistance.

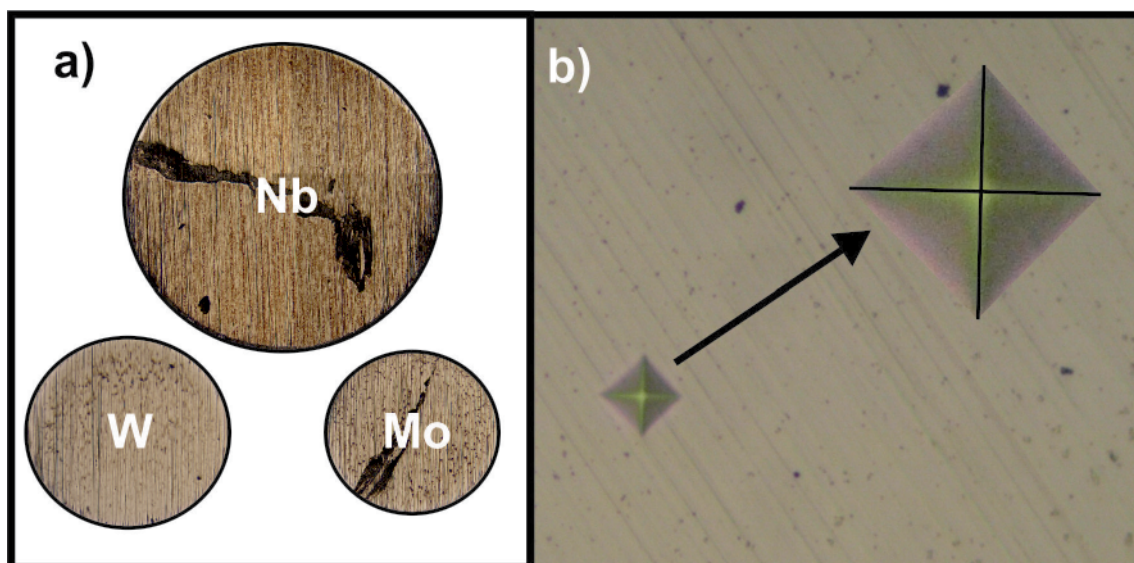


Fig. 5. a) Images of the abrasion test for the investigated alloys, b) Exemplar image of the microhardness test for the plate-form sample of  $\text{Fe}_{61}\text{Co}_{10}\text{Y}_8\text{Nb}_1\text{B}_{20}$

TABLE 3

Results of the microhardness (averaged over 5 measurements) and abrasion tests

Alloy composition	Microhardness [Hv <sub>0.1</sub> ] Averaged over 5 measurements	Surface area [ a.u. ]	Ref.
Fe <sub>61</sub> Co <sub>10</sub> Y <sub>8</sub> Nb <sub>1</sub> B <sub>20</sub>	1185 (±9)	2515 (±50)	—
Fe <sub>61</sub> Co <sub>10</sub> Y <sub>8</sub> W <sub>1</sub> B <sub>20</sub>	1214 (±5)	1006 (±20)	[20]
Fe <sub>61</sub> Co <sub>10</sub> Y <sub>8</sub> Mo <sub>1</sub> B <sub>20</sub>	1180 (±7)	731 (±10)	—

#### 4. Conclusions

The injection casting method facilitated production of Fe<sub>61</sub>Co<sub>10</sub>Y<sub>8</sub>Me<sub>1</sub>B<sub>20</sub> amorphous alloy samples in plate-form (where: Me = Nb, W, Mo). Small additions of non-magnetic elements, such as: Nb, W or Mo, were not found to have changed the thermal stability range of the magnetic properties. The Curie temperatures ( $T_c$ ) for all three of the investigated alloys were comparable (within the error range of ±5 K) and were equal to approximately  $T_c \approx 560$  K.

The investigated materials exhibited very good soft magnetic properties, i.e.: high values of the saturation magnetization ( $\mu_0 M_s$ ) and low values of the coercivity ( $H_c$ ). However, addition of 1% of W was found to significantly decrease the coercivity field to  $H_c = 24$  A/m.

Significant improvements in the mechanical properties were found to have occurred in the alloy containing W, i.e. the highest value of microhardness (1214  $\mu\text{Hv}_{100}$ ) and second highest abrasion resistance within the investigated group of alloys). The highest and lowest values of abrasion resistance were achieved in the alloys with additions with addition of Nb and Mo, respectively.

In summary, it can be concluded that even slight changes in the chemical composition of the investigated alloys can result in significant improvement of their functional parameters. As a result, these slight modifications have to be taken into account during the design process of modern amorphous alloys for selected specialist applications.

#### REFERENCES

- [1] R.W. Cahn, Rapidly solidified alloy, in: H.H. Libermann (Ed.), New York: Marcel Dekker Inc. (1993).
- [2] H. Davies, M. Gibbs, Soft Magnetic Materials, in: K. Kronmuller, S. Parkin (Ed.) Handbook of Magnetism and advanced materials vol. 4. London: John Wiley&Sons; (2007).
- [3] Y. Yoshizawa, S. Oguma, K. Yamauchi, J. Appl. Phys. **64**, 6044 (1988).
- [4] Y. Yoshizawa, K. Yamauchi, Mater. T. JIM **31**, 307 (1990).
- [5] G. Herzer, Acta Mater. **61**, 718 (2013).
- [6] M. Yousefi, Kh. Rahmani, M.S. Amiri Kerahroodi, J. Magn. Magn. Mater. **420**, 204 (2016).
- [7] A. Inoue, Mater. Sci. Eng. **A304-306**, 1 (2001).
- [8] A. Inoue, Acta Mater. **48**, 279 (2000).
- [9] A. Inoue, Mater. T. JIM **36** (7), 866 (1995).
- [10] P. Pietrusiewicz, M. Nabiałek, M. Dośpiał, K. Gruszka, K. Błoch, J. Gondro, P. Brągiel, M. Szota, Z. Stradomski, J. Alloy Compd. **615**, S67 (2014).
- [11] Zubair Ahmad, Mi Yan, Shan Tao, Zhongwu Liu, J. Magn. Magn. Mater. **332**, 1 (2013).
- [12] L.Y. Sheng, J.T. Guo, H.Q. Ye, Materials and Design **30**, 964 (2009).
- [13] ZHAN Yuyong, PAN Jing, JIANG Xiaoli, LIU Xincui, DONG Youren, XIAO Xiaoyan, J. Rare Earth. **33** (10), 1081 (2015).
- [14] J. Hosko, I. Janotova, P. Svec, D. Janickovic, G. Vlasak, E. Illeko-va, I. Matko, P. Svec Sr., J. Non-Cryst. Solids **358**, 1545 (2012).
- [15] Kagan Sarlar, Ilker Kucuk, J. Magn. Magn. Mater. **374**, 607 (2015).
- [16] Hossein Asghari Shivaee, A. Castellero, P. Rizzi, P. Tiberto, Hamid Reza Madaah Hosseini, M. Baricco, Met. Mater. Int. **19** (4), 643 (2013).
- [17] W. H. Wang, Roles of minor additions in formation and properties of bulk metallic glasses, Prog. Mater. Sci. **52**, 540 (2007).
- [18] A. P. Cracknell, Magnetism in Crystalline Materials, Pergamon Press, Oxford, 1975.
- [19] X. Yang, X. Ma, Q. Li, S. Guo, J. Alloy Compd. **S54**, 446 (2013).
- [20] M. Nabiałek, P. Pietrusiewicz, M. Dośpiał, M. Szota, J. Gondro, K. Gruszka, A. Dobrzańska-Danikiewicz, S. Walters, A. Bukowska, J. Alloy Compd. **615**, S56 (2014).
- [21] M. Nabiałek, P. Pietrusiewicz, K. Błoch, J. Alloy Compd. **628**, 424 (2015).
- [22] M. Nabiałek, A. Dobrzańska-Danikiewicz, P. Pietrusiewicz, Z. Stradomski, M. Dośpiał, M. Szota, J. Gondro, S. Lesz, Acta. Phys. Pol. A **126**, 112 (2014).
- [23] T. Egami, Intermetallics **14**, 882 (2006).